In situ measurements of the evolution of young sea ice

Dirk Notz[1,2] and M. Grae Worster[1]

Received 10 May 2007; revised 19 September 2007; accepted 9 November 2007; published 1 March 2008.

[1] We present data from in situ measurements of the salinity evolution of young sea ice in the Arctic. The measurements were carried out with very high vertical and temporal resolution over the course of a few days until the ice had reached a thickness of around 20 cm. The measured bulk salinity profiles show that during ice growth, sea-ice salinity is continuous across the ice-ocean interface and that there is no instantaneous loss of salt at the advancing front. Measured salt fluxes emanating from the ice are as high as 90 g m^{-2} h^{-1} during the first few hours of new ice formation and are roughly half as large during later stages of the experiments. The bulk salinity within the ice decreases continuously with time from the ocean water salinity to a near–steady state value of around 4 parts per thousand (ppt). These results are interpreted with ideas from mushy layer theory using a Rayleigh number to analyze gravity drainage as the driving mechanism for the observed salt loss. In our experiments, gravity drainage occurs for a critical Rayleigh number of around 10, in close agreement with earlier theoretical and experimental studies.

Citation: Notz, D., and M. G. Worster (2008), In situ measurements of the evolution of young sea ice, *J. Geophys. Res.*, *113*, C03001, doi:10.1029/2007JC004333.

1. Introduction

[2] The bulk salinity of sea ice and its temperature determine the ratio of solid, pure ice to interstitial liquid brine, which are the two main components of sea ice. Since the liquid and solid phases have different properties, most small- and large-scale properties of sea ice depend strongly on their relative volume fraction and hence on bulk salinity. For example, the heat conductivity of sea ice with a high solid fraction is more than twice that of warm, salty sea ice with a low solid fraction. The heat capacity of sea ice changes by more than 2 orders of magnitude depending on liquid fraction [*Schwerdtfeger*, 1963; *Ono*, 1967]. Modeling the evolution of bulk salinity and solid fraction profiles realistically is hence important for a proper simulation of the impact of sea ice on the polar and global climate system, which was also underlined by the recent studies of *Feltham et al.* [2006] and *Vancoppenolle et al.* [2005], for example. In addition to the impact of the bulk salinity field on the properties of the sea ice itself, the loss of salt from sea ice can cause significant changes in the underlying water masses and can trigger deep thermobaric convection [see, e.g., *McPhee*, 2000].

[3] Despite the importance of the bulk salinity of sea ice, to our knowledge there exist no data sets of high-resolution, in situ measurements of its evolution in natural sea ice, mostly for want of a technique that would lend itself to carry out such measurements in the field. Such measurements have, however, been carried out in laboratory experiments [e.g., *Cox and Weeks*, 1975; *Shirtcliffe et al.*, 1991; *Aussillous et al.*, 2006]. Here we present results from in situ measurements of bulk salinity and temperature profiles that were made in two experiments in very young sea ice in the Arctic. We have used a new instrument that is capable of such measurements [*Notz et al.*, 2005], which we describe briefly in section 2. In section 3 we show the measured evolution of the salinity field. The results are discussed in section 4, focusing on the functioning of gravity drainage as the main physical mechanism leading to the loss of salt from sea ice during winter.

2. Instrumental Setup

[4] The instrument we used, which is described in detail by *Notz et al.* [2005], consists of thin, horizontal, platinum wires, which are spanned in pairs with a horizontal spacing of 5 mm at each depth at which the solid fraction is to be measured. Our instrument consists of 14 such pairs, which are located between 0.5 and 17 cm below the ice surface with a vertical spacing of between 0.5 cm toward the top and 2 cm toward the bottom. The length of the wires and hence the horizontal distance over which sea-ice properties are averaged is 15 cm. By measuring the electrical impedance between the two wires of each pair, it is possible to calculate the average solid volume fraction ϕ_v of the sea ice along the wires, from which the solid mass fraction ϕ_m can be derived. The measurement relies on the fact that the pure solid ice is a very good insulator whereas the interstitial

[1]Institute of Theoretical Geophysics, Department of Applied Mathematics and Theoretical Physics, University of Cambridge, Cambridge, UK.
[2]Max Planck Institute for Meteorology, Hamburg, Germany.

0148-0227/08/2007JC004333

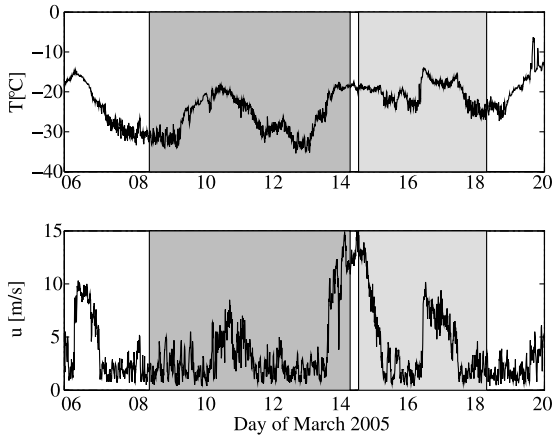

Figure 1. Air temperature T and 10-min averaged wind speed u at 4 m height during the field experiments. The duration of the two experiments is indicated by the shaded areas. The data stem from the weather station in Adventdalen, Svalbard, 4 km away from the measuring site, and have kindly been provided by the University Centre in Svalbard.

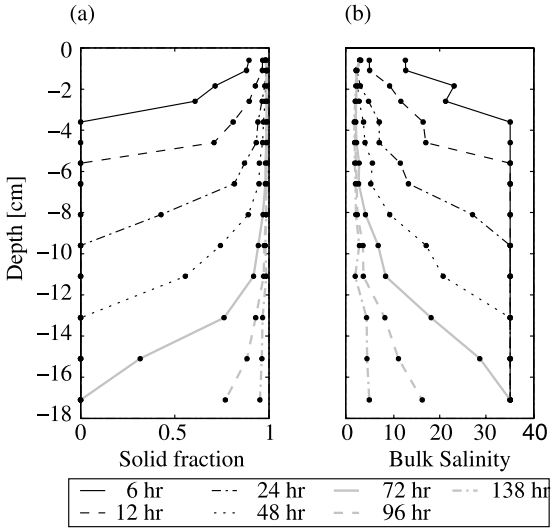

Figure 2. Profiles of (a) the solid fraction and (b) the bulk salinity at different times during the first field experiment described in this paper.

brine is a good conductor. Thermistors are mounted on the instrument at the levels of the wire pairs to measure the temperature profile in the ice. The salinity of the interstitial brine S_{br} depends only on this temperature [e.g., *Cox and Weeks*, 1986] and can be combined with the measured solid mass fraction ϕ_m to give the bulk salinity profile of sea ice according to

$$S_{bu} = S_{br}(1 - \phi_m). \quad (1)$$

Tests of the instrument under controlled laboratory conditions gave results in very good agreement with analytical and numerical predictions [*Notz et al.*, 2005].

3. Measured Data

[5] In March 2005 we used this instrument to carry out two experiments to measure the evolution of the bulk salinity of growing natural sea ice in situ. The measurements took place on land-fast sea ice in Adventfjorden in Svalbard at roughly 78°N. Since the instrument must be deployed in open water, we cut a 1 × 1 m hole into the relatively smooth, about 50-cm-thick land-fast ice that covered the fjord when we started our experiment. The instrument measured the salinity of the new ice as it formed in this hole over the course of a few days.

3.1. Experiment 1

[6] During the first experiment the weather was very stable, with cold air temperatures and little wind (Figure 1). The average air temperature during the 6-d-long duration of this experiment was −26.1°C, with a minimum value of −35.4°C and a maximum value of −17.5°C. Hence ice growth started very rapidly in the hole, and the full 17-cm measuring depth of our instrument was covered in ice after less than 4 d. Figure 2a shows the vertical profiles of solid fraction, and Figure 2b shows the bulk salinity for various times during this experiment. Apart from the last two profiles, for which the ice had grown farther than our instrument reached, all solid fraction profiles show zero solid fraction at the ice-ocean interface (Figure 2a). From thermodynamic considerations it follows that the temperature field and hence the brine salinity field are continuous across the interface as well, which is also confirmed by the smoothness of the temporal traces of our temperature measurements that are shown in Figure 3. It therefore follows from equation (1) that the bulk salinity directly at the interface must be equal to that of seawater (Figure 2b).

[7] The salinity profiles all tend toward an almost uniform bulk salinity of around 4 ± 1 parts per thousand (ppt) throughout most of the upper parts of the ice, and there is no increase in salinity toward the top of the ice as is the case in the C-shaped salinity profile that is often measured in young sea ice [e.g., *Nakawo and Sinha*, 1981]. The reason for this lies most likely in the very calm initial growth conditions, as will be discussed in section 4.

[8] The salt loss at different levels in the ice as a function of time is shown in Figure 4. The bulk salinity is shown at

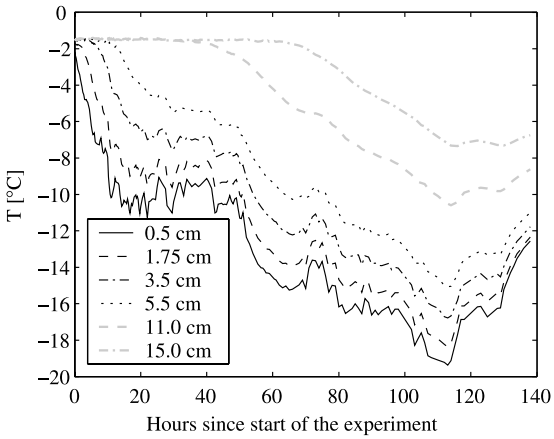

Figure 3. Temporal evolution of the temperature field at various levels in the first experiment.

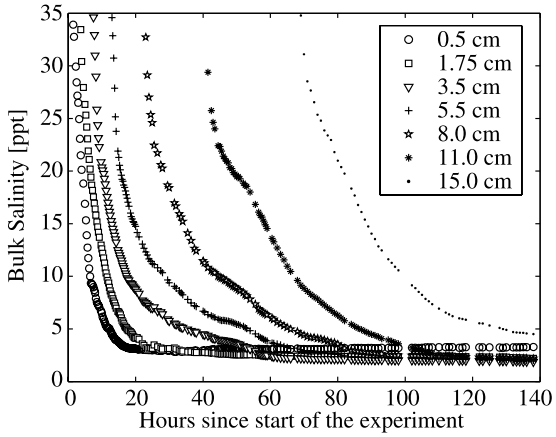

Figure 4. Temporal evolution of the bulk salinity at various depths during the first field experiment.

every other wire pair as measured by our instrument. Figure 4 shows clearly the relatively rapid but never instantaneous loss of salt from sea ice. During the rapid development of the initial very thin ice, most of the salt is lost within 24 h. In the slower-growing ice the desalination rate is much smaller, and it takes several days until the bulk salinities have dropped to a near–steady state value of below 5 ppt. Figure 5 shows the temporal evolution of the mean salinity of the full 17-cm-deep layer in which the instrument is measuring. The continuous measurement of the development of the mean bulk salinity of the sea ice is difficult in that no continuous ice thickness measurements are available. However, the total salt flux into the underlying ocean can be calculated from the slope of the mean salinity of the full 17-cm column that is shown in Figure 5. After rapid desalination of about 90 g m^{-2} h^{-1} in the initial 24 h the desalination rate became much smaller (40 g m^{-2} h^{-1}) and remained almost constant roughly until 80 h into the experiment. Afterward, no further assessment of the salt

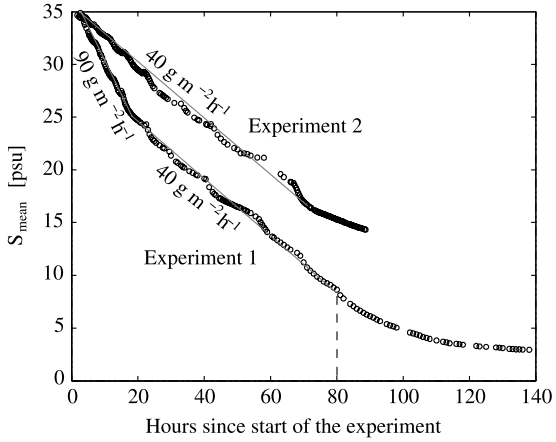

Figure 5. Temporal evolution of the mean bulk salinity of the upper 17 cm of the water column that is governed by the instrument during both field experiments. The thin lines are approximate linear fits to the data and indicate salinity fluxes as labeled. The dashed line indicates the time at which the full instrument was covered by ice in the first experiment.

flux from the forming sea ice is possible, since it had grown across the instrument and the salt flux emanating from the sea ice growing below the instrument cannot be measured. These comparatively high salt fluxes were caused by the high ice growth rates, which were due to the cold air temperatures and the absence of any insulating snow on top of the ice. Such conditions can arise in nature during the initial refreezing of leads in the pack ice cover, for example.

[9] Despite the very low solid fraction close to the interface, which goes along with a relatively low heat conductivity, the temperature profiles that we measured are surprisingly linear throughout almost the full ice thickness (see Figure 6). The spacing of our thermistors is most likely too large to resolve the change in the temperature gradient that one would expect to go along with the change in heat conductivity. We have therefore used the time traces of temperature that are shown in Figure 3 for the determination of the onset of ice formation at a certain thermistor [cf. *Wettlaufer et al.*, 2000]. Ice thicknesses derived in this way are in very good agreement with those derived from changes in the impedance of the wire pair at a certain depth. They are shown for the two experiments as a function of time since the start of the experiment in Figure 7. The determination of the onset of ice formation at a wire pair is important because the impedance just before this time acts as the reference value from which solid fraction and hence bulk salinity are derived with our instrument. Note that the thermistors at 6.5 and 8 cm failed during the experiment, which is why no temperature data are available from these levels. For the calculation of the bulk salinity, the temperature profiles were interpolated with cubic fits at these levels.

[10] Between roughly hours 45 and 55 of the experiment, the surface temperature of the ice started to decrease significantly. This went along with an increase in ice growth rate, as can be seen from the deviation from the square root profile that roughly governs the early ice thickness evolution shown in Figure 7. This episode also goes along with increasing desalination at all levels, as shown by the relatively sudden change in curvature around this time in Figures 4 and 5. Such changes in ice surface temperature might therefore be of relevance for the general evolution of sea-ice salinity.

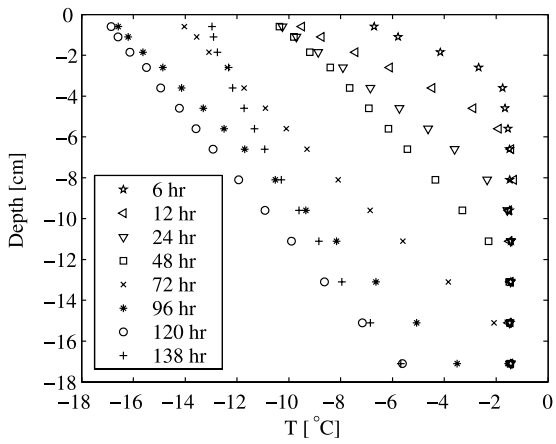

Figure 6. Temperature profiles at various times during the first experiment.

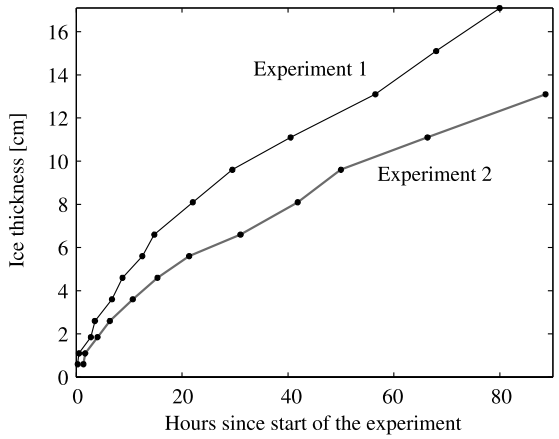

Figure 7. Evolution of the ice thickness as a function of time during both field experiments. The ice thickness was determined whenever the advancing front reached a wire pair.

[11] Under-ice currents and tides might also have some impact [*Feltham et al.*, 2002]. We note that a correction to those theoretical results [*Neufeld et al.*, 2006] suggests that there is little or no direct influence of under-ice shear on the interior evolution of the mushy layer, but more recent results (J. Neufeld and J. S. Wettlaufer, private communication, 2006) show that under-ice shear in concert with buoyancy can significantly affect the onset of gravity drainage. However, we have no means to assess these effects given our data.

[12] It is also interesting to note that the bulk salinity at the uppermost wire pair (5 mm below the ice surface) seems to increase very slightly by 0.3 ppt from its minimum value until the end of the experiment. This increase might be caused by internal redistribution of brine within the sea ice caused by internal density changes (so-called brine expulsion) or by percolation of some of the thin high-salinity surface layer that had formed on top of the ice at the beginning of the experiment.

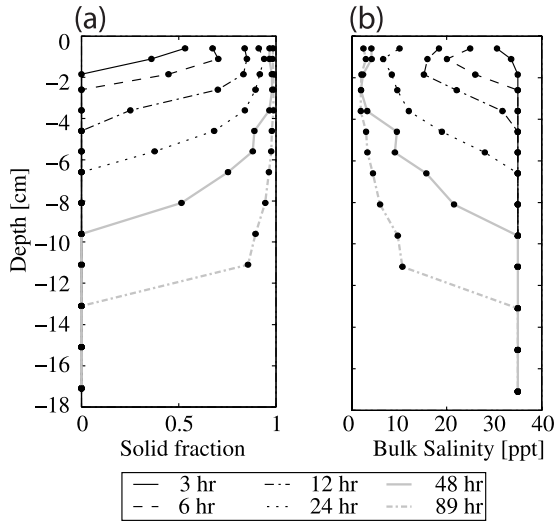

Figure 8. Profiles of (a) the solid fraction and (b) the bulk salinity at different times during the second field experiment described in this paper.

3.2. Experiment 2

[13] The second experiment was started on a very windy day, with maximum wind gusts of 18 m s^{-1} (Figure 1). Therefore the water in the hole that was used for the measurements was initially very well mixed, which led to frazil ice formation. Conditions were hence more comparable to new ice formation in the open ocean or a wind-driven polynya. The wind speeds decreased rapidly over the first 24 h, and the period with a well-mixed water column and frazil ice formation was very short. The mean air temperature during the 4-d-long duration of the second experiment was −20.2°C, with a maximum value of −14.1°C and a minimum value of −26.9°C.

[14] The early salinity profiles shown in Figure 8b show some resemblance to a C shape, which, however, is not present in the later cores. This initial C shape is probably caused by brine that is embedded between the initially formed frazil ice crystals. Since the period with high wind speeds was very short, the frazil ice layer was probably relatively thin (1–2 cm) and the brine could drain very efficiently out of it once the ice had started to consolidate. This might not be the case if the frazil ice layer had become thicker before consolidation, as it does under open-ocean conditions.

[15] The temporal evolution of the bulk salinity at various depths is shown in Figure 9. Because of the different initial growth conditions with lower growth rates (see Figure 7), salt loss occurs generally more slowly than in the first experiment. It takes, for example, almost 48 h for the salinity of the uppermost wires to decrease to values below 5 ppt. As is apparent from Figure 5, the salt flux in the second experiment is rather constant throughout the whole measurement period and lacks the initially fast desalination that was apparent in the first experiment. Its magnitude is about 40 g m^{-2} h^{-1}, comparable to that of the first experiment after the initial fast desalination.

4. Discussion

[16] In winter the temperature of sea ice generally decreases toward its surface. This temperature gradient goes along with a brine salinity gradient, because in order to maintain phase equilibrium the salinity of the interstitial

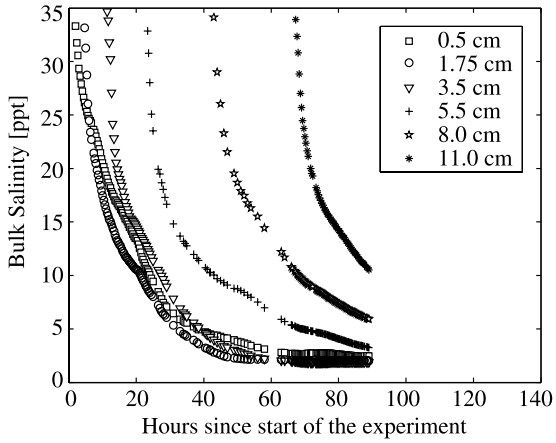

Figure 9. Temporal evolution of the bulk salinity at various depths during the second field experiment.

liquid brine always adjusts itself such that it remains at the local liquid temperature. Since lower temperatures correspond with higher brine salinities, and since the brine density is mostly controlled by brine salinity, the liquid brine in sea ice during winter is unstably stratified and is prone to convective overturning. Such overturning, or gravity drainage as it is usually called, is shown by *Notz* [2005] and Notz and Worster (Desalination processes of first-year sea ice, submitted to Journal of Geophysical Research, 2008) to be the only mechanism by which significant amounts of salt are lost from sea ice during winter. The contribution of other processes that have previously been suggested is negligible: So-called brine expulsion caused by internal phase changes only leads to a redistribution of salt within the ice, since the downward velocity of the salt can be shown to be always less than the ice growth velocity at the interface. Diffusion of salt within the interconnected brine network and of individual brine pockets can be shown to be too slow to contribute significantly to the salt loss from sea ice, mostly because the gradient in the brine salinity is mostly governed by the temperature gradient, which is comparably weak in sea ice [see also *Untersteiner*, 1968].

[17] The classical assumption that the bulk of the salt loss from sea ice occurs by salt rejection directly at the advancing ice-ocean interface can be ruled out both because of our measurements and because of theoretical considerations employing mushy layer theory: Such salt rejection would imply a jump in the salinity field across the ice-ocean interface, which cannot occur in growing sea ice since both the solid fraction and the temperature fields must be continuous across the advancing front [*Worster*, 2002; *Notz*, 2005]. This is also partly confirmed by our measurements. The impedance measurements show no sign of discontinuity when the ice-ocean interface passes the level of a wire pair and the corresponding thermistor. Here this interface is defined as the lowermost level at which the temperature lies more than 0.05°C below the far-field temperature. Given that the impedance of each wire pair is strongly controlled by the immediate surroundings of the individual wires, the impedance that we measure at that level is representative of the solid fraction at the ice-ocean interface on a millimeter scale in the vertical. On that scale we find continuity in solid fraction. Since it follows both from the smoothness of the temporal traces of the temperature evolution (Figure 3) and from thermodynamical considerations that the temperature field and therefore the brine salinity are continuous across the interface as well, the bulk salinity field must also be continuous across the interface. We hence focus in the following on gravity drainage as the only process that can in our opinion explain the temporal evolution of the salinity field that was measured by our instrument.

[18] Such analysis can be carried out by employing the concept of a mush Rayleigh number *Ra* [*Worster*, 1992, 2000; *Wettlaufer et al.*, 1997], which describes the susceptibility of sea ice to gravity drainage. A local Rayleigh number can be written as

$$Ra = (h - z)\frac{g\rho_l\beta\Delta S_{br,z}\Pi\left(\phi_{v,\max}\right)}{\kappa\mu}, \qquad (2)$$

where $h-z$ is the distance between the ice-ocean interface at depth h and the level z in the ice, g is the acceleration due to gravity, $\rho_l\beta\Delta S_{br,z}$ is the difference between the density of seawater and that of brine at level z, κ is thermal diffusivity, μ is the dynamic viscosity of the liquid, and $\Pi(\phi_{v,\max})$ is the effective permeability of the ice as a function of the maximum solid volume fraction $\phi_{v,\max}$ between the level z and the ice-ocean interface. The physical interpretation of this Rayleigh number is that convection can only occur if the driving buoyancy given by the brine density gradient expressed in the numerator is large enough to overcome dissipation as expressed by the denominator. This Rayleigh number is essentially a porous-medium Rayleigh number [*Phillips*, 1991] but is somewhat peculiar in that although the driving buoyancy is dominated by the gradient in brine salinity, the dissipation depends primarily on the thermal field. This is because the thermal field determines the brine salinity of the convecting brine. The direct impact of temperature on brine density is negligible compared to the impact of the brine salinity (see *Worster* [2000] and *Notz* [2005] for details). Whenever the value of this Rayleigh number exceeds a critical value Ra_c, convection will start. The convection causes salty brine to drain out of the ice, which leads to a decrease in the overall bulk salinity and, according to equation (1), to an increase in solid fraction, which in turn lowers the value of *Ra*.

[19] For the functional dependence of $\Pi(\phi_v)$, we use the empirical relationship

$$\Pi = 10^{-17}\left[10^3(1-\phi_v)\right]^{3.1} \qquad (3)$$

that was found for young sea ice by *Freitag* [1999]. The functional form of this relationship is very similar to the theoretically derived Kozeny equation, according to which $\Pi = 0.667(1-\phi_v)^3/M^2$ in a porous medium with capillaries made up of thin strips, where M is the total interstitial surface area of the pore space per unit volume [e.g., *Bear*, 1988]. The permeability of sea ice during summer that is calculated using this expression is comfortably within the range measured by *Eicken et al.* [2002], indicating that equation (3) might also be a good approximation for the average permeability of older ice.

[20] Figure 10a shows Rayleigh number profiles calculated according to equations (2) and (3) for various times during the first experiment, taking the bulk salinity as constant at 35 ppt. In this case the permeability of the sea ice remains relatively high, and strongly supercritical Rayleigh numbers can develop, i.e., Rayleigh numbers above about 10. In such cases, convection would penetrate the whole layer of sea ice. In contrast, Figure 10b shows the Rayleigh number profiles that have actually developed during the first experiment calculated using the measured salinity evolution. In contrast to the fictive high-salinity case shown in Figure 10a, significant convection can only occur in the lowest part of the sea ice, since only there is *Ra* supercritical. The driving brine density difference from the ocean is higher the higher up one gets into the ice, but owing to the low salinity, the permeability in the top part of the ice is too low at later stages of the experiment to allow the Rayleigh number to be large enough for the convection to reach into these upper regions. We suggest this is why the

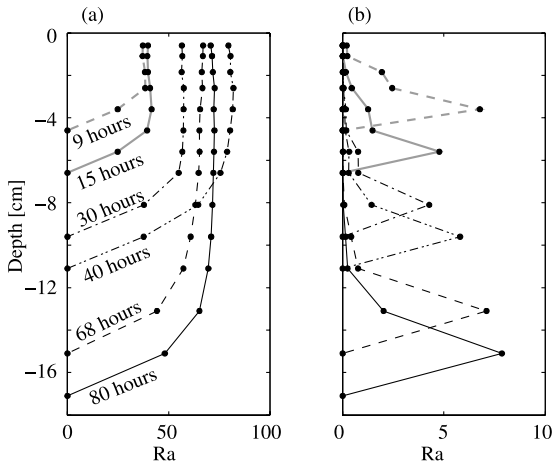

Figure 10. Vertical profiles of the mush Rayleigh number *Ra* at various times during the first experiment (a) if no salt would have been lost from the forming sea ice and (b) for the measured salinity evolution. The labels indicate the time that has passed since the beginning of the experiment. Note the different scaling of the *x* axes.

salinity reaches a lower limit of around 3–4 ppt, beyond which it does not decrease any further in our experiment. Quantitatively, it is interesting to note that the value of the maximum Rayleigh number remains rather constant throughout the experiment and lies in the range that has also been suggested by other theoretical and experimental studies, namely, at around 10 [e.g., *Worster*, 1992; *Tait and Jaupart*, 1992]. This indicates that *Ra* does not usually exceed Ra_c significantly but that the change in the solid fraction that is caused by the convection lowers *Ra* such that it remains close to its critical value.

[21] In laboratory experiments a delay of the initial release of salt from newly forming sea ice has been found [*Wettlaufer et al.*, 1997]. These experiments were carried out in closed tanks, where the cooling plate at the top of the tank was in direct contact with the salt water in the tank. In this way the surface temperature was fixed to a certain value, and the ice forming initially had a relatively low brine fraction because of its low temperature. Hence the Rayleigh number was below its critical value until the ice had reached a certain thickness and gravity drainage could set in. In the field experiments described in this paper, however, such delay in the initial salt release was all but absent. The reason for this is that the surface temperature in natural sea ice decreases only slowly after the initial ice formation (see Figure 7), which is why the initially forming ice is relatively warm and hence permeable enough to allow for gravity drainage even at very low ice thickness. In another field study [*Wettlaufer et al.*, 2000], conditions were such that a delay in the onset of gravity drainage was inferred and was found to be consistent with measurements of salinity in the underlying water column.

[22] In our experiments the salinity near the ice surface is relatively low compared with previous studies in Arctic first-year sea ice, which often show a significant salinity increase toward the surface. This difference is probably caused by the fact that sea ice usually forms under rather turbulent conditions, with a relatively high bulk salinity of the initial frazil-seawater mixture. Once this slushy mixture consolidates, the vertical permeability of the forming granular ice, having predominantly vertical c axes, is most likely much lower than that in the columnar ice that forms under calm growth condition. The consolidated layer of low-permeability ice might under natural conditions often be too thick for gravity drainage to lead to efficient desalination at all levels, which could explain the higher salinities that are often found in sea ice toward the surface. Laboratory experiments aiming to find useful parameterizations to describe the loss of salt from sea ice might therefore profit from being carried out in open tanks in which the surface temperature can adjust in a similar way as in the field and initial frazil ice formation can occur.

5. Conclusion

[23] In this paper we have presented results from in situ measurements of the bulk salinity evolution of natural sea ice. The measurements confirm that the salinity field is continuous across the ice-ocean interface and that salt loss is a continuous process that is driven by the brine density gradient that is usually present in the ice during winter. This brine density gradient can cause convectional overturning of brine, so-called gravity drainage, which can be examined by employing the concept of a mush Rayleigh number. Our measurements indicate that an actively convecting zone exists in the lowest few centimeters of natural sea ice, with a mush Rayleigh number remaining close to its critical value of around 10. If this observation were confirmed through further experimental and theoretical studies, it might guide the way to a dynamically based parameterization of salt loss from sea ice caused by gravity drainage. In this way the salinity evolution of sea ice could be modeled more realistically in large-scale models than is currently the case. With an expected increase in first-year sea-ice cover in the Arctic, understanding the initial desalination processes of sea ice might well have a significant large-scale impact.

[24] **Acknowledgments.** The field work described in this paper would not have been possible without the logistical support that we received from the University Centre on Svalbard (UNIS), especially from F. Nilsen. This support is gratefully acknowledged. We also thank R. Style for his help in the field. We particularly thank John Wettlaufer for introducing M.G.W. to Arctic fieldwork, for his leading involvement in the development of the profiler, and for numerous fruitful discussions. We also thank two anonymous reviewers who helped to improve this paper significantly. This work was made possible by support from the National Environmental Research Council under grant NER/B/S/2002/00521 (D.N. and M.G.W.) and the Studienstiftung des Deutschen Volkes (D.N.), which are both very gratefully acknowledged.

References

Aussillous, P., A. J. Sederman, L. F. Gladden, H. E. Huppert, and M. G. Worster (2006), Magnetic resonance imaging of structure and convection in solidifying mushy layers, *J. Fluid Mech.*, *552*, 99–125.

Bear, J. (1988), *Dynamics of Fluids in Porous Media*, Dover, New York.

Cox, G. F. N., and W. F. Weeks (1975), Brine drainage and initial salt entrapment in sodium chloride ice, *CRREL Res. Rep. 345*, U.S. Army Cold Reg. Res. and Eng. Lab., Hanover, N. H.

Cox, G. F. N., and W. F. Weeks (1986), Changes in the salinity and porosity of sea-ice samples during shipping and storage, *J. Glaciol.*, *32*, 371–375.

Eicken, H., H. R. Krouse, D. Kadko, and D. K. Perovich (2002), Tracer studies of pathways and rates of meltwater transport through Arctic summer sea ice, *J. Geophys. Res.*, *107*(C10), 8046, doi:10.1029/2000JC000583.

Feltham, D. L., M. G. Worster, and J. S. Wettlaufer (2002), The influence of ocean flow on newly forming sea ice, *J. Geophys. Res.*, *107*(C2), 3009, doi:10.1029/2000JC000559.

Feltham, D. L., N. Untersteiner, J. S. Wettlaufer, and M. G. Worster (2006), Sea ice is a mushy layer, *Geophys. Res. Lett.*, *33*, L14501, doi:10.1029/2006GL026290.

Freitag, J. (1999), Untersuchungen zur Hydrologie des arktischen Meereises—Konsequenzen für den kleinskaligen Stofftransport (in German), *Ber. Polarforsch. 325*, Alfred Wegener Inst. fuer Polar und Meeresforsch., Bremerhaven, Germany.

McPhee, M. G. (2000), Marginal thermobaric stability in the ice-covered upper ocean over Maud Rise, *J. Phys. Oceanogr.*, *30*, 2710–2722.

Nakawo, M., and N. K. Sinha (1981), Growth rate and salinity profile of first-year sea ice in the high Arctic, *J. Glaciol.*, *27*, 315–330.

Neufeld, J. A., J. S. Wettlaufer, D. L. Feltham, and M. G. Worster (2006), Corrigendum to flow-induced morphological instability of a mushy layer, *J. Fluid Mech.*, *549*, 442–443, doi:10.1017/S002211200500813X.

Notz, D. (2005), Thermodynamic and fluid-dynamical processes in sea ice, Ph.D. thesis, Univ. of Cambridge, Cambridge, U. K.

Notz, D., J. S. Wettlaufer, and M. G. Worster (2005), A non-destructive method for measuring the salinity and solid fraction of growing sea ice in situ, *J. Glaciol.*, *51*, 159–166.

Ono, N. (1967), Specific heat and heat of fusion of sea ice, in *Physics of Snow and Ice*, vol. 1, edited by H. Oura, pp. 599–610, Inst. of Low Temp. Sci., Sapporo, Japan.

Phillips, O. M. (1991), *Flows and Reactions in Permeable Rocks*, Cambridge Univ. Press, New York.

Schwerdtfeger, P. (1963), The thermal properties of sea ice, *J. Glaciol.*, *4*, 789–807.

Shirtcliffe, T. G. L., H. E. Huppert, and M. G. Worster (1991), Measurements of the solid fraction in the crystallisation of a binary melt, *J. Crystal Growth*, *113*, 566–574.

Tait, S., and C. Jaupart (1992), Compositional convection in a reactive crystalline mush and melt differentiation, *J. Geophys. Res.*, *97*, 6735–6756.

Untersteiner, N. (1968), Natural desalination and equilibrium salinity profile of perennial sea ice, *J. Geophys. Res.*, *73*, 1251–1257.

Vancoppenolle, M., T. Fichefet, and C. M. Bitz (2005), On the sensitivity of undeformed Arctic sea ice to its vertical salinity profile, *Geophys. Res. Lett.*, *32*, L16502, doi:10.1029/2005GL023427.

Wettlaufer, J. S., M. G. Worster, and H. E. Huppert (1997), Natural convection during solidification of an alloy from above with application to the evolution of sea ice, *J. Fluid Mech.*, *344*, 291–316.

Wettlaufer, J. S., M. G. Worster, and H. E. Huppert (2000), Solidification of leads: Theory, experiment, and field observations, *J. Geophys. Res.*, *105*, 1123–1134.

Worster, M. G. (1992), Instabilities of the liquid and mushy regions during solidification of alloys, *J. Fluid Mech.*, *237*, 649–669.

Worster, M. G. (2000), Solidification of fluids, in *Perspectives in Fluid Dynamics*, edited by M. G. W. G. K. Batchelor and H. K. Moffatt, pp. 393–446, Cambridge Univ. Press, Cambridge, U. K.

Worster, M. G. (2002), Interfaces on all scales during solidification and melting, in *Interfaces for the 21st Century*, edited by M. K. Smith et al., pp. 187–201, Imperial College Press, London.

D. Notz, Max Planck Institute for Meteorology, Bundesstraße 53, D-20146 Hamburg, Germany. (dirk.notz@zmaw.de)

M. G. Worster, Institute of Theoretical Geophysics, Department of Applied Mathematics and Theoretical Physics, University of Cambridge, Wilberforce Road, Cambridge CB3 0WA, UK.